Geomechanics and Engineering, *Vol. 30, No. 4 (2022) 325-336*
https://doi.org/10.12989/gae.2022.30.4.325

Analysis of surface settlement troughs induced by twin shield tunnels in soil: A case study

Chang-Yoon Ahn[1,2a], Duhee Park*[1] and Sung-Woo Moon[3b]

[1]*Department of Civil and Environmental Engineering, Hanyang University, 222 Wangsimni-ro, Sageun-dong, Seongdong-gu, Seoul, Korea*
[2]*HDC Hyundai Development Company, 55, Hangang-daero 23-gil, Yongsan-gu, Seoul, Korea*
[3]*Department of Civil and Environmental Engineering, Nazarbayev University, 53 Kabanbay Batyr Ave, Nur-Sultan 010000, Kazakhstan*

(*Received September 3, 2021, Revised July 3, 2022, Accepted July 18, 2022*)

Abstract. This paper analyzes the ground surface settlements induced by side-by-side twin shield tunnels bored in sedimentary soils, which primarily consist of sand with clay strata above the tunnel crown. The measurements were obtained during the construction of twin tunnels underneath the Incheon International Airport (IIA) located in Korea. The measured surface settlement troughs are approximated with Gaussian functions. The trough width parameters i and K of the settlement troughs produced by the first and second tunnel passings are determined, along with those for the total settlement trough. The surface settlement troughs produced by the first shield passing are reasonably represented by a symmetric Gaussian curve. The surface settlement troughs induced by the second shield tunnel display marginal asymmetric shapes at selected sections. The total settlement troughs are fitted both with a shifted symmetric Gaussian function and the superposition method utilizing an asymmetric function for the incremental trough produced by the second tunnel. It is revealed that the superposition method does not always produce better fits with the total settlement. Instead, the shifted symmetric Gaussian function is overall demonstrated to provide more favorable agreements with the recordings. Therefore, the shifted symmetric Gaussian function is recommended to be used in the design for the prediction of the settlement in clays caused by twin tunneling considering the simplicity of the procedure compared with the superposition method. The amount of increase in the width parameter K for the twin tunnel relative to that for the single tunnel is quantified, which can be used for a preliminary estimate of the surface settlement in clay induced by twin shield tunnels.

Keywords: asymmetrical function; shifted Gaussian curve; surface settlement trough; trough width parameter; twin shield tunnel

1. Introduction

With the global trend of urbanization, the demand for new underground infrastructures including pipelines and tunnels, as well as building foundations, is increasing. The metro and road tunnels are being built to connect metropolitan areas and alleviate congested traffic. With an increase in the utilization of underground space, new tunnel excavations adjacent to existing underground structures have become common. One of the primary concerns of tunneling adjacent to existing structures is the control of settlement during excavation. The surface settlement profile is most often approximated as a Gaussian distribution function, as proposed by Peck (1969) based on field measurements.

The shapes of settlement troughs induced by shield tunneling have been widely studied (Mair *et al*. 1993, O'reilly and New 1982, Rankin 1988). In particular, Mair *et al*. (1993) presented a method to estimate the subsurface settlement trough induced by a single tunnel based on the centrifuge test data of Mair (1979) and a wide range of field measurements (Attewell and Farmer 1974, Barratt and Tyler 1976, Glossop 1978, Stallebrass *et al*. 1992). Chou and Bobet (2002) proposed an analytical solution and compared the observed and predicted settlement troughs measured from 28 sections of 14 single shield tunnels in clay. Zapata (1998) compared the measured settlements induced by shield tunnels in clay and numerical analysis outputs. Liao *et al*. (2009), Chakeri *et al*. (2013), Ding *et al*. (2017) studied the effect of shield tunneling adjacent to existing structures through numerical simulations. McCabe *et al*. (2012) analyzed the measured maximum settlements and volume losses produced by single tunnelling in Irish glacial tills. Xu *et al*. (2011) conducted laboratory model tests and presented relationships between soil deformation and various operating parameters of shield machine in silty clay.

The surface settlement troughs induced by twin shield tunnels have also been reported in a number of studies (Chen *et al*. 2018, Djelloul *et al*. 2018, Fargnoli *et al*. 2015, Jin *et al*. 2018, Kim *et al*. 2020, Li and Yuan 2012, Nawel and Salah 2015, Suwansawat and Einstein 2007, Xu *et al*. 2011). Suwansawat and Einstein (2007) provide extensive investigations of the measured surface settlement troughs over side-by-side and stacked earth pressure balanced

*Corresponding author, Professor
E-mail: dpark@hanyang.ac.kr
[a]Ph.D. Student
E-mail: hycivileng@hanyang.ac.kr
[b]Assistant Professor
E-mail: sung.moon@nu.edu.kz

ISSN: 2005-307X (Print), 2092-6219 (Online)

(EPB) twin tunnels constructed primarily in clays. For side-by-side twin tunnels, it was reported that the settlement troughs after the first shield passing are symmetric. However, the troughs produced by the second shield passing yield different shapes including symmetric and asymmetric curves. A superposition technique was proposed to predict the total settlement trough, where the troughs caused by first and second shield passings are separately fitted, after which they are summed. It was reported that the second shield passing settlement trough can be approximated with a symmetric Gaussian curve. It should be noted that because the chamber pressure applied was significantly increased during the second passing to reduce the settlement, the pattern of observed settlement troughs is likely to be quite different from that produced by twin tunnelling where similar levels of chamber pressures are applied to both first and second shield passings. Sirivachiraporn and Phienwej (2012) studied the settlement troughs over twin tunnels constructed primarily in stiff and soft Bangkok clays. However, the settlement troughs induced by the second shield passing were not investigated in detail. Della Valle and Rodríguez (2014) proposed an asymmetric Gaussian functional form to fit the settlement trough induced by the second shield passing. However, the trend of the settlement trough shapes yielded by the second tunnel passing was not extensively studied. In contrast to the measurements of Suwansawat and Einstein (2007), the second shield passing produced a significantly larger settlement trough compared with that caused by the first shield passing. Zhao *et al*. (2019) presented the influence between the tunnel depth and spacing of twin tunnels on the settlement troughs in sand through numerical simulations. The literature review illustrates that a consensus on how to predict the settlement trough induced by twin tunnels has not yet been reached.

The objective of the paper is to propose an ideal procedure to estimate the settlement trough induced by twin shield tunnels. To this end, the measured surface settlement troughs produced by twin shield tunnels in sands and clays are studied. The shapes of the surface settlement troughs produced by the second shield tunneling relative to those induced by the first shield tunneling are compared. Recommendations are provided on how to predict the settlement troughs over twin shield tunnels. Additionally, the amount of increase in the empirical width parameter of the settlement trough for the twin shield tunnels relative to that for the single tunnel is quantified. The purpose of this process is to provide a preliminary estimate of the surface settlement in clay induced by twin shield tunnels.

2. Predictive methods for estimation of tunneling induced settlement trough

Peck (1969) reported, based on field recordings, that the surface settlement profile induced by a single tunnel can be well fitted by a Gaussian distribution function, as shown in Fig. 1. The settlement was represented as

$$\delta = \delta_{\max} \exp\left[\frac{-x^2}{2i^2}\right] \tag{1}$$

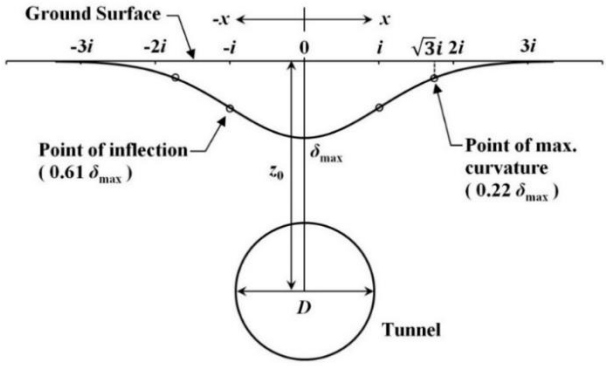

Fig. 1 Surface settlement profile (modified after Peck 1969)

where δ is the surface settlement at distance x from tunnel centerline, $\delta_{\max}$ is the maximum surface settlement, and i is the trough width parameter. i is defined as the distance from the centerline of a tunnel to the inflection point of the settlement trough.

Peck (1969) reported that the settlement trough of twin tunnels can also be fitted by a Gaussian function if the twin tunnels are located close to each other. New and Bowers (1994) presented that an improved fit with the asymmetric settlement trough can be achieved for twin tunnels by introducing an offset distance Δx as follows

$$\delta_t = \delta_{\max,t} \exp\left[\frac{-(x \pm \Delta x)^2}{2i_t^2}\right] \tag{2}$$

where δ_t is the surface settlement of twin tunnels at a distance x from the twin tunnels centerline, $\delta_{\max,t}$ is the maximum surface settlement, i_t is the trough width parameter in twin tunnels. Δx represents the distance from the centerline to the location at which $\delta_{\max,t}$ occurs.

The asymmetric settlement trough of twin tunnels can also be best represented using a superposition principle. The settlement troughs for the first and second shield passings are separately calculated, after which they are summed to obtain the total settlement. This procedure is described as follows

$$\begin{aligned}\delta_t = {} & \delta_{\max,1st} \exp\left[\frac{-(x - \Delta x_{1st})^2}{2i_{1st}^2}\right] \\ & + \delta_{\max,2nd} \exp\left[\frac{-(x + \Delta x_{2nd})^2}{2i_{2nd}^2}\right]\end{aligned} \tag{3}$$

where δ_t is the surface settlement caused by twin tunnels at distance x from the centerline, $\delta_{\max,i}$, i_i, Δx_i are the maximum surface settlement, trough width parameter, and offset distance produced by tunnel i, respectively.

The superposition technique can be categorized into three methods based on the assumption of the shape of the settlement trough produced by the second shield passing. In the first method, it is assumed that the settlement trough induced by the second tunnel is identical to that produced by the first tunnel (O'reilly and New 1982). For this procedure, $i_{1st}=i_{2nd}$, $\delta_{\max,1st}=\delta_{\max,2nd}$, and $\Delta x_{1st}=\Delta x_{2nd}$. In the second method, two symmetric settlement troughs with different shapes for first and second tunnel excavations, respectively, are superposed (Suwansawat and Einstein

(a) A route map of AREX

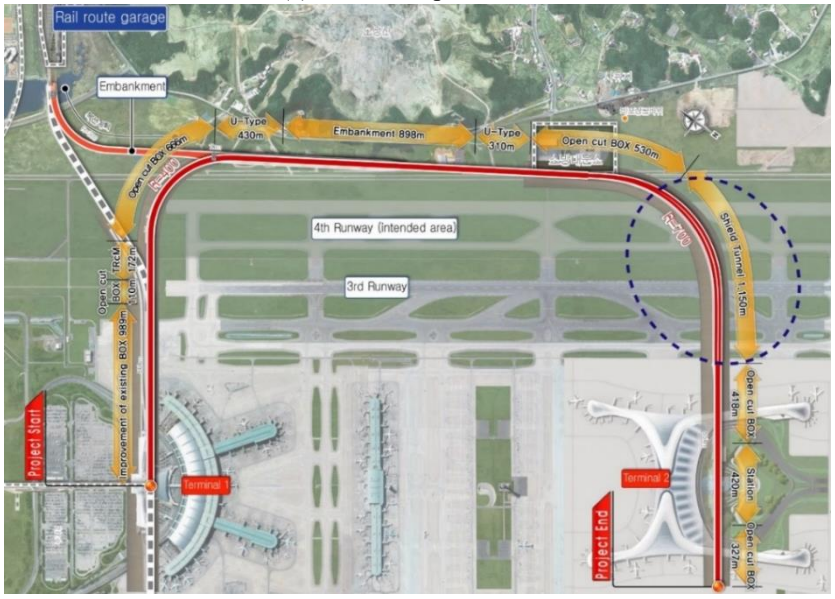

(b) The location of shield tunnel (after Ahn (2017))

Fig. 2 Plan of T1-T2 rail road construction

Table 1 Empirical equations correlating i with z_0 for single tunnel

Model	Functional form
Peck (1969)	$i = \left(\frac{D}{2}\right) \cdot \left(\frac{z_0}{D}\right)^n, n = 0.8 \sim 1.0$
O'reilly and New (1982)	$i = 0.43z_0 + 1.1$
Herzog (1985)	$i = 0.40z_0 + 1.92$
Arioglu (1992)	$i = 0.40z_0 + 0.60$

2007). The parameters for Eq. (3) differ for the first and second tunnels, respectively. In the third method, an asymmetrically shaped settlement trough is assumed to be produced by the second tunnel, as reported in various studies (Chapman *et al*. 2004, Della Valle and Rodríguez 2014). For this asymmetric trough, the settlement curve is split into two limbs. i_{2nd} of the half trough facing the first tunnel, referred to as i_n, is greater than that of the half trough facing the remote-field, termed as i_r. This is attributed to the loosening of soil around the first tunnel, producing higher deformation and wider troughs. It was presented that the additional settlement trough can be well approximated with an asymmetric Gaussian curve, applying different width parameters i_n and i_r to two half troughs.

A series of empirical equations that related i with the depth of tunnel center z_0 have been proposed for clay profiles, as summarized in Table 1. For practical purposes, i can also be estimated from the following empirical equation (Mair *et al*. 1993)

$$i = K \cdot z_0 \tag{4}$$

where K is an empirical parameter. O'reilly and New (1982) and Rankin (1988) reported that a reasonable estimate for K is 0.5 for single tunnels constructed in clays. Mair and Taylor (1997), Suwansawat and Einstein (2007), Sirivachiraporn and Phienwej (2012) and McCabe *et al*. (2012) presented that K ranges from 0.4 to 0.6 for clays. Considerng the narrow range of K, it was also reported that for most cases K can be set as 0.5 irrespective of clay type, as recommended by Rankin (1988).

The volume per unit length of the surface settlement trough (V_s) can be calculated by integration of Eq. (1) as follows

$$V_s = \sqrt{2\pi} \cdot i \cdot \delta_{\max} \tag{5}$$

The volume loss (or ground loss) V_L is the ratio of V_s to the excavated face area, usually expressed as a percentage. It is calculated as follows for a shield tunnel with a diameter of D

$$V_L = \frac{4V_s}{\pi D^2} \tag{6}$$

3. Project overview

3.1 General information

The Incheon International Airport (IIA), located in the

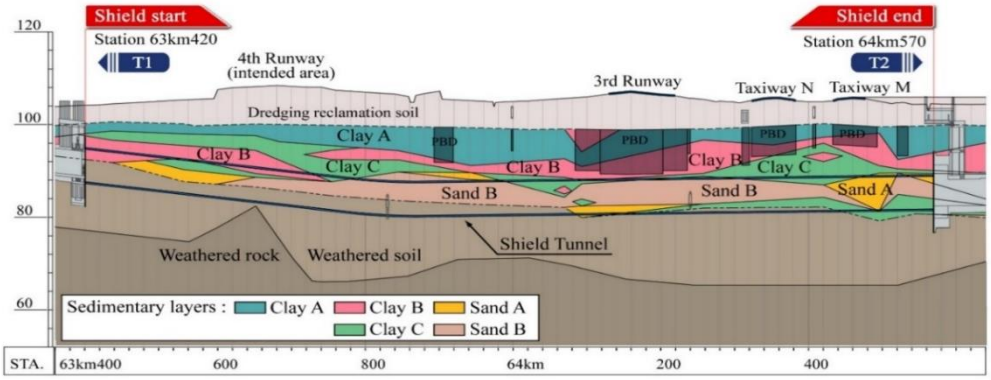

Fig. 3 Ground conditions of the shield tunnel

Table 2 Soil properties

Soil properties	Clay A (soft)	Clay B (stiff)	Clay C (very stiff)
USCS	ML-CL	CL, ML	CL, ML
N_{60}	4	8	17
γ_t (kN/m^3)	18.5	19.4	19.9
s_u (kPa)	30.0	45.0	100.0
ϕ ($^\circ$)	0	0	0
E (MPa)	3.83	7.20	11.50
Poisson's ratio	0.40	0.35	0.35
c_{cu} (kPa)	14.0	16.0	16.0
ϕ_{cu} ($^\circ$)	12.0	16.0	16.0

Yellow Sea of Korea (Fig. 2), is the main international airport in Korea. The second passenger terminal (T2) of IIA was newly constructed to accommodate rapidly increasing air traffic demands. Because Airport Railroad Express (AREX) only runs from the Seoul station to the first passenger terminal (T1) of IIA, a T1-T2 railroad was newly constructed to provide a transport service connecting T1 and T2. The total length of T1-T2 railroad is 6.36 km. The shield tunnel of T1-T2 railroad crosses the 3rd runway and taxiways (named N, M) of IIA, which were in full operation during the construction of the tunnel, as shown in Fig. 2(b). The shield tunnel is composed of 2 tubes where the length of tunnel 1 is 1,150 m and the length of tunnel 2 is 1,127 m. The depth of the shield tunnel gradually increases with tunneling and maintains a constant depth from the start to the end of the third runway section (Fig. 3). The depth of shield tunnel center ranges from 13.3 to 22.3 m, whereas the center span of the twin tunnels ranges from 11.4 to 20.8 m (Ahn 2017, Korea-National-Railway 2013). The twin shield tunnels were sequentially constructed with one piece of EPBs TBM. The first shield tunnel was excavated from T1 towards T2. After the shield TBM was u-turned, the second shield tunnel was excavated from T2 towards T1.

3.2 EPBs TBM and engineering geology

The shield tunnel for the railroad in this project has an outer diameter of 7.77 m and an inner diameter of 7.07 m. The earth pressure balance shield (EPBs) TBM was manufactured to minimize the settlement of the operating runway and taxiway. The diameter of EPBs TBM is 7.91 m and the excavation diameter of the cutter is 7.93 m. In order to minimize the gap between EPBs TBM and cutting surface, the cutter head was designed in the flat face spoke type which the opening ratio is 60%. The gap between the machine's skin and the ground's cutting surface is only 2 mm. The tail void between the segment concrete and the cutting surface is only 16 mm. The tail void is continuously filled with the cement grout, simultaneously advancing the EPBs TBM. Also, the mixing ratio of cement grout was designed to have a quick setting and enough liquidity to fill the tail void. The EPBs TBM was applied with a total of 30 jacks for the thrust force and a total of 14 motors for the rotation of cutter head. The max. total thrust force of shield jacks is 60 MN and the advance speed of jacks is 0.06 m/min. The max. torque of cutter head is 12,620 kN-m and the max. revolution per minute (RPM) is 1.5.

The IIA, where is the test site of this study, was built on a reclaimed island. The bedrock of the site is composed of Jurassic biotite granite. Because the Yellow Sea, where IIA is located, is shallow and has a large tidal range of approximately 9 m, a thick sedimentary layer has been formed as shown in Fig. 3. The stratified soil profile consists of alternating layers of clays and sands. The clay has a high silt content and is predominantly composed of kaolinite. Clay A~C is from soft to very stiff clay and their USCS is classified as ML-CL. Sand A is classified as SM and sand B is classified as SP. N-value is 4/50 in clay A, 8/50 in clay B, 17/50 in clay C, and 21/50 in sand. The excavated soil properties are summarized in Table 2. As shown in Fig. 3, the shield TBM was excavated through clay, sand, and weathered soil layers. The primary excavation was performed through the sand layer, with portions of clay layer scattered around the upper part of the shield tunnel. The groundwater level was located between elevation levels of 99 and 102 m in Fig. 3.

4. Field measurements

To secure safe and uninterrupted aircraft service, rigorous settlement management of both runway and taxiway during and after the tunnel excavation was critical. A suite of instruments was installed to monitor the surface settlements, as shown in Figs. 4 and 5. The surface settlements were measured at a total of 22 sections, which

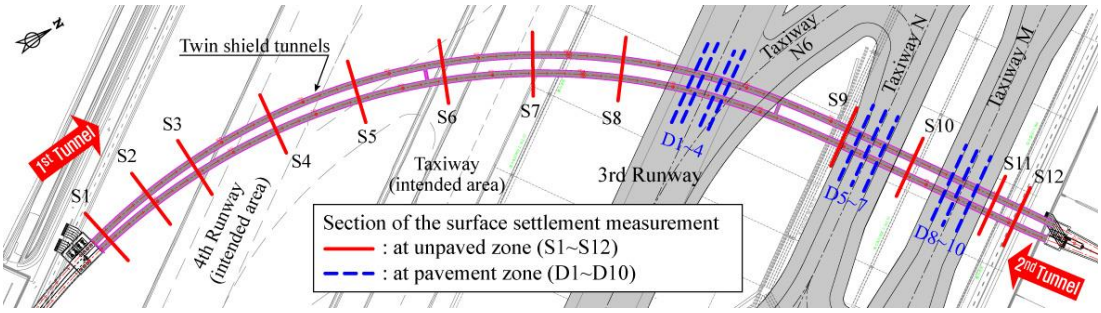

Fig. 4 Measurement sections of the surface settlement trough

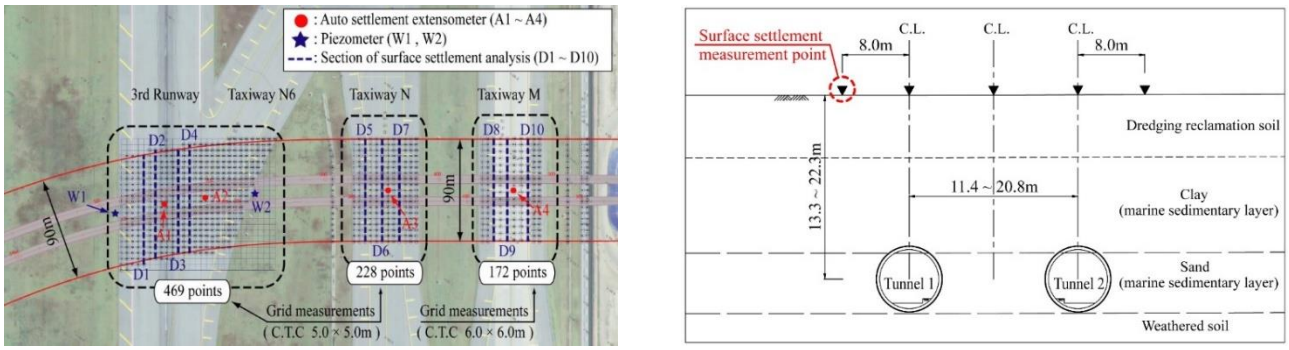

(a) Pavement zone (D1 ~ D10) (b) Unpaved zone (S1 ~ S12)

Fig. 5 Details of the measurements in Fig. 4

include 10 measurements above the third runway and taxiway pavements and 12 recordings on unpaved green zones.

The settlements on unpaved zones were measured at five points per section, as shown in Fig. 5(b). During the excavation underneath the third runway and taxiway, the shield TBM was operated 24 hours a day without a break time. Auto settlement extensometers were installed to measure the real-time surface and subsurface settlement, the locations of which are denoted as A1 to A4 in Fig. 5(a). Additionally, detailed surface settlement measurements at grid spacings of 5 to 6 m were carried within a width of 90 m around the twin shield tunnels on paved sections, denoted as D1 to D10, as shown in Fig. 5(a). Because the settlement arrays were only installed above the pavement, only the sections D1~D10 were used to analyze the surface settlement profile.

5. Analysis of field measurement results

In this section, the results of Gaussian functions fitted to the measured settlement troughs are presented. The parameter i is calculated by reformulating Eq. (1) as follows

$$\ln\frac{\delta}{\delta_{\max}} = -\frac{x^2}{2i^2} = -\frac{1}{2K^2}\left(\frac{x}{z_0}\right)^2 \tag{7}$$

Linear regression was used to obtain i that produces the best fit with the measurements. The parameter K was calculated as $K = i/z_0$, as shown in Fig. 6. The i and K pairs were determined for the 22 measurement sections (S1~S12 and D1~D10) using the above procedure, the details of which are presented in the following.

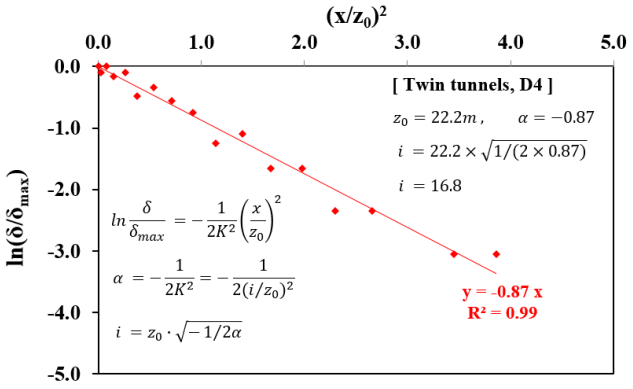

Fig. 6 Example of estimating the settlement trough width parameter

In this study, two types of settlement troughs were developed. The first type settlement trough was developed using the asymmetric superposition method. In the procedure, a symmetric Gaussian function was initially fitted to the settlement trough produced by the first tunnel passing. The resulting parameter that yields the best fit with the single tunnel is denoted as K_s. Then, the settlement trough induced by second tunnel passing was matched with the asymmetric trough function presented by Della Valle and Rodríguez (2014) using the parameters K_n and K_r. The K_n and K_r are parameters for the near-field and remote-field limbs of the second tunnel settlement trough as defined in Fig. 7. This second tunnel passing induced settlement trough was back-calculated by subtracting the first passing induced settlement from the total settlement (Suwansawat and Einstein 2007), as shown in Fig. 7.

The second type of the trough was developed to fit the

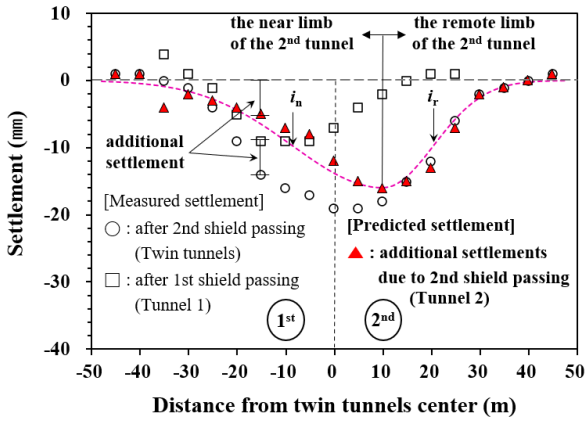

Fig. 7 Procedure for back-calculating the additional settlement induced by the second shield passing. Also shown are the definitions of the near-field and remote-field limbs of the asymmetric settlement trough

total settlement after second tunnel passing using the shifted symmetric Gaussian function, the best fit parameter of which is termed as K_t. The fitted curves are compared with the recordings in Figs. 8 and 9.

The surface settlement troughs induced by first shield passings are reasonably well represented by Gaussian curves, where the maximum surface settlements are shown to occur around the tunnel centerline. The settlement troughs produced by second tunnel passings overall display marginal asymmetric shapes, and therefore are well fitted using variable parameters K_n and K_r. The total settlement troughs produced by twin tunnels are compared with two sets of fitted curves. Both the predicted troughs using K_t and K_n & K_r are displayed. It is revealed that the K_n & K_r based curves do not always yield an enhanced fit with the total settlement. On the contrary, it may produce wider curves than the measured settlement troughs above the second tunnel, as seen in D1, D2, D8, D9, and D10. The shifted Gaussian curves developed from K_t provide reasonable estimates for all cases. To quantify the accuracy of the estimated settlement troughs, the error rates of predicted V_L are compared with measurements in Table 3. The error rates of the symmetric curves utilizing K_t are revealed to be lower compared with those obtained using the superposition procedure at all sections except for D3. The fit with the recorded V_L are quite remarkable, resulting in less than 10% residual. This comparison highlights that the use of the shifted symmetric Gaussian curves is reliable for the prediction of the settlement induced by twin tunnels. The superposition method was not applied for S1~S12 sections, because of difficulties in developing the second passing induced incremental settlement trough using only five measurements per section. They were therefore only fitted with the shifted symmetric function, from which K_t are extracted, as shown in Fig. 10. The surface settlements of S1~S12 are shown to be well fitted with the shifted symmetric Gaussian curves.

Table 4 summarizes the estimated empirical parameter K of the twin tunnels, including K_s, K_t, and K_n & K_r. The ratios of the second tunnel related parameters K_t and K_n & K_r with

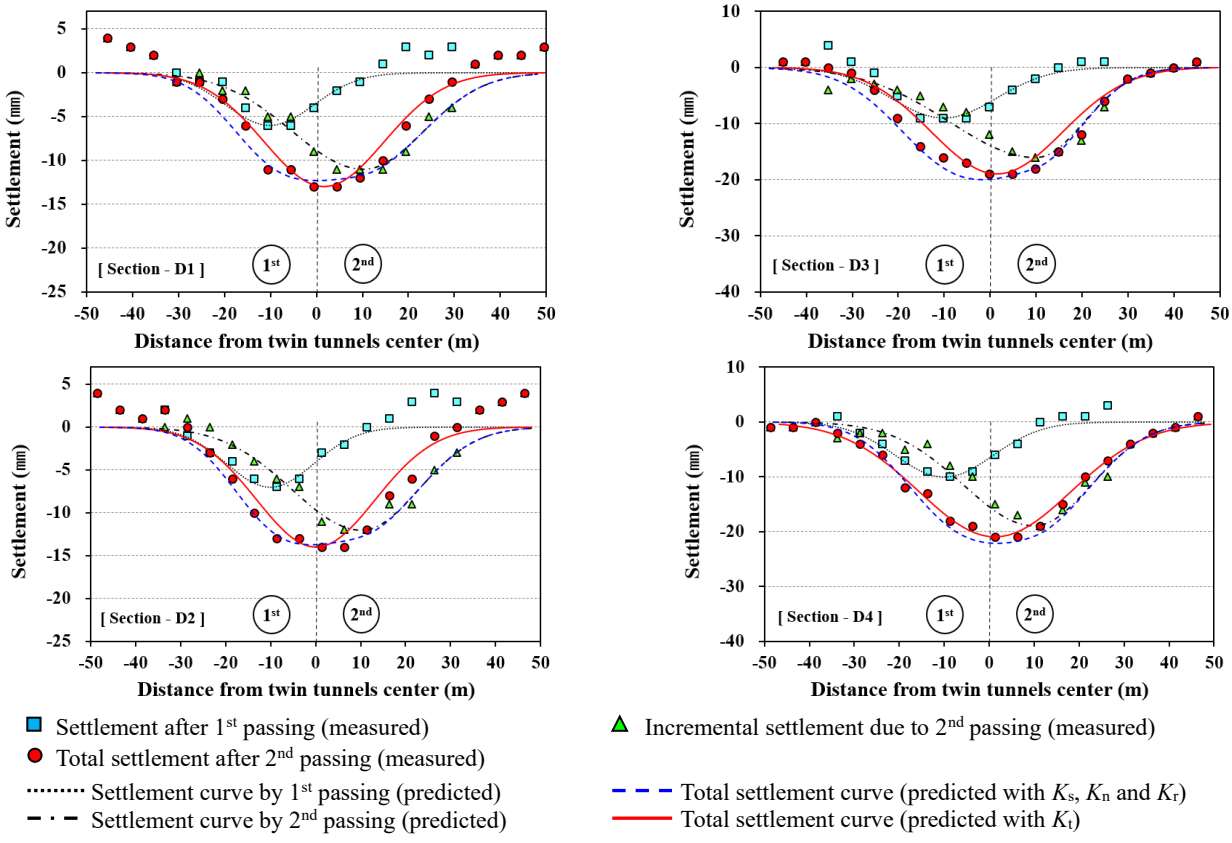

Fig. 8 Comparison of measured settlements in D1~D4 and fitted curves

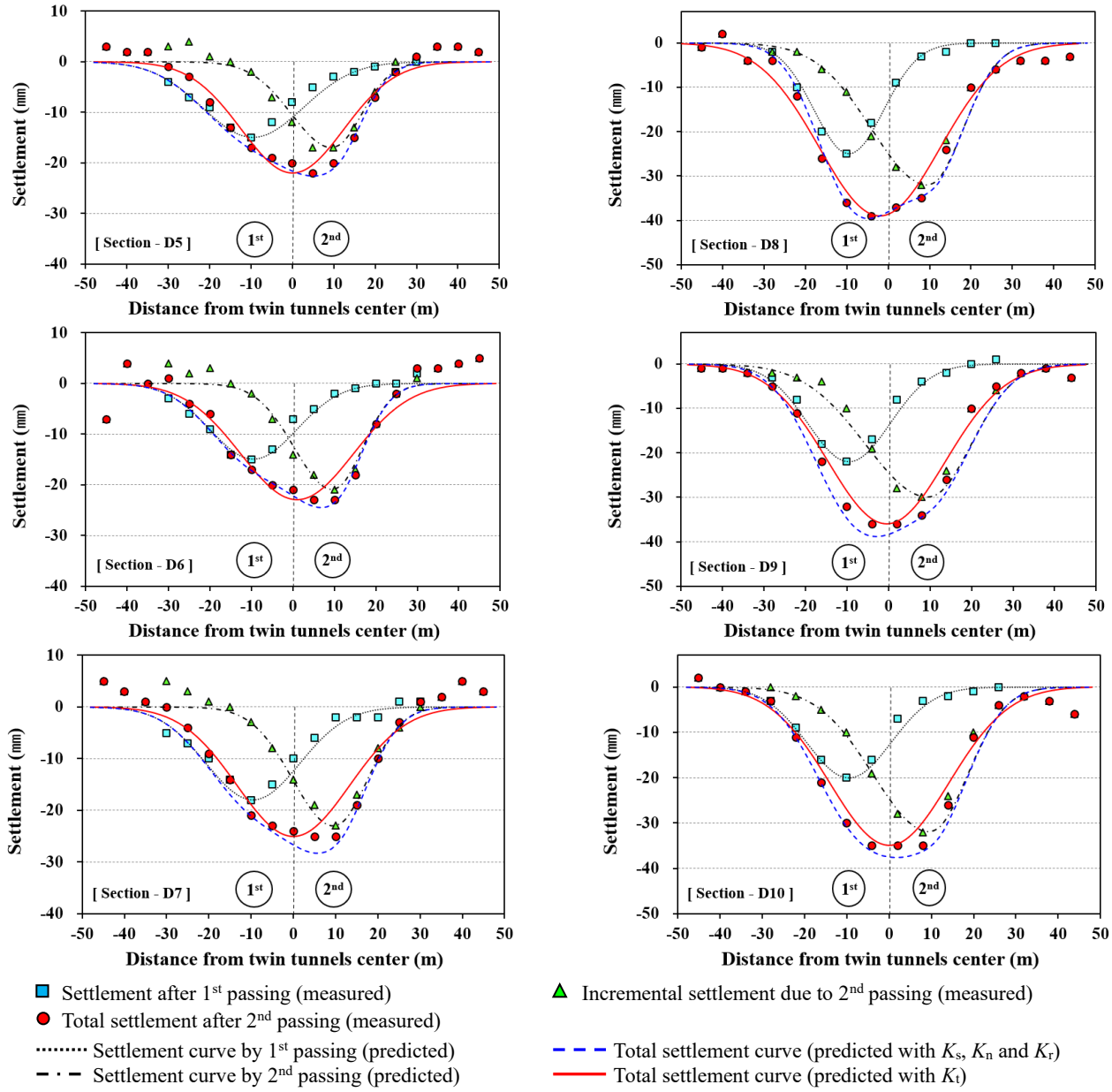

Fig. 9 Settlement measured in D5 ~ D10, and comparison of fitting curves

Table 3 Volume loss and error rate of settlement trough in twin tunnels

No.	Volume loss, V_L (%)			Error rate for measured V_L	
	Measured value	Super-position method	Shifted symmetric curve	Super-position method	Shifted symmetric curve
D1	0.46	0.55	0.43	16.4%	7.0%
D2	0.51	0.60	0.47	15.0%	8.5%
D3	0.77	0.85	0.69	9.4%	11.6%
D4	0.88	0.96	0.90	8.3%	2.2%
D5	0.74	0.83	0.69	10.8%	7.2%
D6	0.78	0.84	0.79	7.1%	1.3%
D7	0.89	1.03	0.85	13.6%	4.7%
D8	1.45	1.43	1.44	1.4%	0.7%
D9	1.35	1.52	1.30	11.2%	3.8%
D10	1.30	1.42	1.25	8.5%	4.0%

respect to the single tunnel parameter are also calculated and listed. The parameter K_s for single tunnels ranges from 0.41 to 0.59, with a mean of 0.49. The values of K are shown to be consistent with those (K=0.5 for clays) reported in O'reilly and New (1982) and Rankin (1988). This is because the settlement dominantly occurred in the clay layer above the tunnel crown, although the shield tunnel was primarily excavated in the sand layer. The parameter K_t for twin tunnels increases from 0.59 to 0.76, with an average of 0.66. The average K_t/K_s ratio is 1.347, which means that the settlement trough width increases by approximately 34.7% for twin tunnels compared with single tunnels. For this particular case study, the ratios fall within a narrow band with a standard deviation of the ratio is 0.19. As observed in the Figures, the near-field limbs are shown to be wider compared with remote-field limbs. The average of K_n is higher than K_s at 0.64, whereas the remote-field

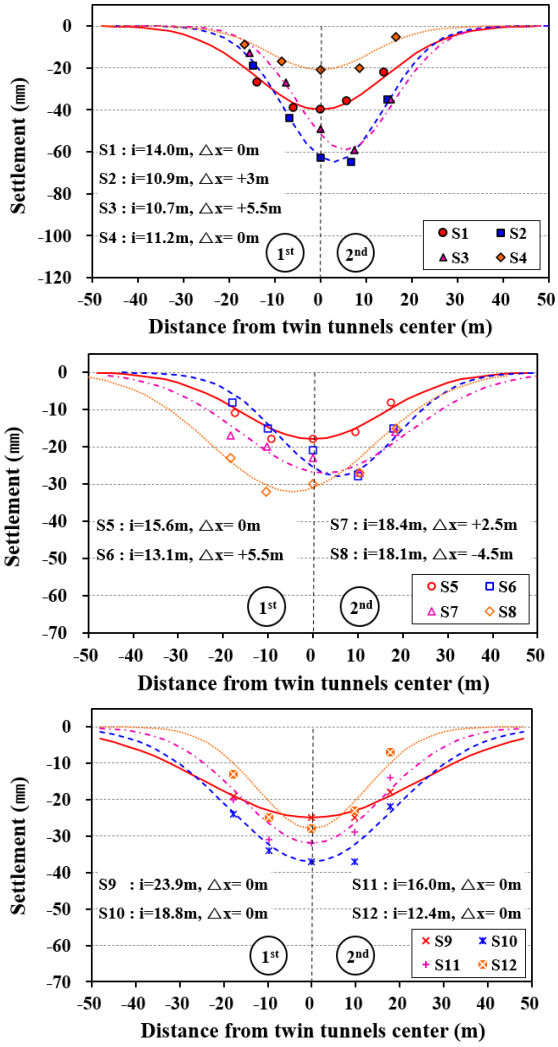

Fig. 10 Surface settlement troughs described by Gaussian curves in unpaved zone after the 2nd shield passing

limb is similar to K_s at 0.46. As discussed in the previous section, such an asymmetric curve is produced by the soil loosening around the first tunnel.

To evaluate the variability of this ratio for similar soil types and different tunnel separation distance, the measured K_s, K_t, and K_n & K_r from the Bangkok MRT project provided in Suwansawat and Einstein (2007) are also listed in Table 4. The parameters K_n & K_r for the Bangkok MRT project in Table 4 were determined in this study from the settlement troughs provided in Suwansawat and Einstein (2007).

The parameter K_s are shown to be larger than those derived in this study, probably because the dominant soil type is soft clay. The average K_t/K_s ratio is 1.237, which is smaller than that calculated in this study. The mean of K_t/K_s ratio for this case study and the Bangkok MRT measurments is approximately 1.3. Although this ratio may change depending on the soil type and tunnel dimension, it can be used as a preliminary estimate considering the similarity of the ratios from two different cases.

In addition to the the Bangkok MRT case, the settlement measurements induced by side-by-side twin tunnels in soft

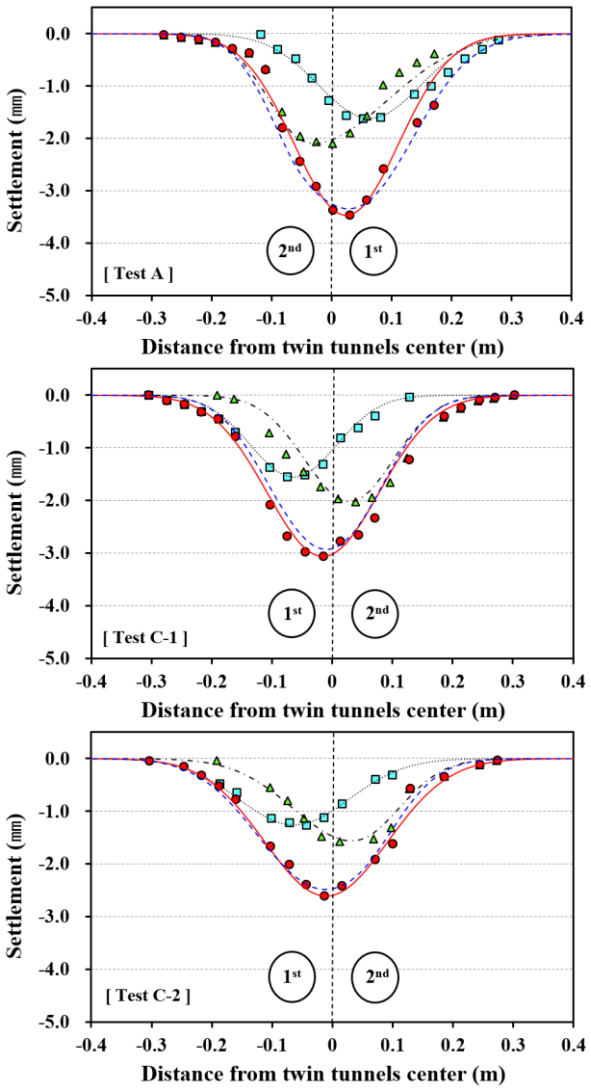

Fig. 11 Settlement troughs measured by the model tests (Chapman *et al*. 2007) and comparison with fitted curves

ground from a laboratory model test (Chapman *et al*. 2007) are shown in Fig. 11. Consistent characteristics are observed, which include the unsymmetrical settlement troughs and the greater settlement above the second tunnel. The settlements measured by laboratory tests in Fig. 11 are extremely similar to the settlement troughs shown in Figs. 8 and 9. They are well fitted by both shifted symmetric and asymmetric curves. The parameter K_s, K_t, K_n & K_r are listed in Table 4.

Fig. 12 plots the relationship between the parameters i and z_0 after second tunnel passing for both D1~D10 and S1~S12 sections. It should be noted that the slope of the relationship represent the parameter K_t. For comparison

Table 4 Parameter K of Tunnel 1, 2 and twin tunnels

Project	Section No.	z_0 (m)	Measured volume loss, V_L(%)			Tunnel 1	Tunnel 2		Twin tunnels		
			Tunnel 1	Tunnel 2	Twin	K_s	K_n	K_r	K_t	Δx (m)	R_{ctc}
T1-T2 Tunnel	D1	22.0	0.25	0.75 (300.0%)	0.46 (184.0%)	0.44	0.71 (161.4%)	0.59 (134.1%)	0.59 (134.1%)	+ 1.7	2.63
	D2	21.2	0.32	0.80 (250.0%)	0.51 (159.4%)	0.44	0.70 (159.1%)	0.57 (129.5%)	0.59 (134.1%)	-	2.62
	D3	22.4	0.46	1.15 (250.0%)	0.77 (167.4%)	0.51	0.84 (164.7%)	0.46 (90.2%)	0.64 (125.5%)	+ 1.5	2.59
	D4	22.2	0.51	1.31 (256.9%)	0.88 (172.5%)	0.49	0.71 (144.9%)	0.57 (116.3%)	0.76 (155.1%)	+ 1.3	2.58
	D5	20.6	0.83	0.75 (90.4%)	0.74 (89.2%)	0.59	0.48 (81.4%)	0.35 (59.3%)	0.60 (101.7%)	-	2.47
	D6	20.8	0.76	0.90 (118.4%)	0.78 (102.6%)	0.50	0.44 (88.0%)	0.35 (70.0%)	0.65 (130.0%)	+ 1.0	2.47
	D7	20.7	0.96	0.97 (101.0%)	0.89 (92.7%)	0.54	0.47 (87.0%)	0.39 (72.2%)	0.64 (118.5%)	-	2.46
	D8	20.5	1.07	1.91 (178.5%)	1.45 (135.5%)	0.41	0.66 (161.0%)	0.41 (100.0%)	0.71 (173.2%)	- 2.0	2.46
	D9	20.7	0.99	1.73 (174.7%)	1.35 (136.4%)	0.48	0.73 (152.1%)	0.50 (104.2%)	0.69 (143.8%)	- 0.5	2.46
	D10	20.5	0.93	1.65 (177.4%)	1.30 (139.8%)	0.49	0.65 (132.7%)	0.44 (89.8%)	0.69 (140.8%)	-	2.46
	Average					0.49	0.64 (130.6%)	0.46 (93.9%)	0.66 (134.7%)		
Bangkok MRT	A : 23-AR-001	22.0				0.68	0.42 (61.8%)	0.51 (75.0%)	0.77 (113.2%)	+ 2.0	1.08
	B : 26-AR-001	18.5				0.70	0.79 (112.9%)	0.60 (85.7%)	0.97 (138.6%)	+ 4.0	1.59
	C : CS-8B	19.0				0.63	0.66 (104.8%)	-	0.74 (117.5%)	- 3.0	1.29
	C : CS-8D	20.1				0.50	0.48 (96.0%)	0.38 (76.0%)	0.65 (130.0%)	- 1.0	1.17
	D : SS-5T-52e-s	22.2				0.59	0.61 (103.4%)	0.41 (69.5%)	0.77 (130.5%)	-	1.61
	D : SS-5T-52e-o	26.0				0.54	0.44 (81.5%)	0.28 (51.9%)	0.65 (120.4%)	-	1.20
	A : 23-G3-007-019	19.0				0.47	0.68 (144.7%)	0.30 (63.8%)	0.58 (123.4%)	+ 8.0	1.58
Lab. test (1g) (Chapman *et al.* 2007)		Test A	0.200 (2.5D)			0.43	0.64 (148.8%)	0.35 (81.4%)	0.44 (102.3%)	25mm	1.60
		Test C-1	0.160 (2.0D)			0.45	0.46 (102.2%)	0.45 (100.0%)	0.58 (128.9%)	-15mm	1.60
		Test C-2	0.224 (2.8D)			0.41	0.44 (107.3%)	0.34 (82.9%)	0.45 (109.8%)	-10mm	1.60
Average (Excluding laboratory test results)						**0.53**	**0.62 (117.0%)**	**0.44 (83.0%)**	**0.69 (130.2%)**		

purposes, the measurements from the Bangkok MRTA project presented in Suwansawat and Einstein (2007) and the model tests (Chapman *et al*. 2007) summarized in Table 4 are also shown. It is a common practice to normalize both should be noted that both i and z_0 are normalized i and z_0 by D and the centerline distance R for single and twin tunnels, respectively. In this study, the parameters are normalized to the tunnel separation distance ratio (R_{ctc}), which is defined as R/D. Except for S1, S4 and S9, the parameter K_t in Fig. 12 ranges from 0.6 to 1.0.

6. Relation between volume loss and operating parameters of EPBs TBM

In soil, the maximum settlement and extent of the settlement trough induced by EPBs TBM are affected by the operational parameters such as chamber pressure, penetration ratio, grouting pressure, and filling (Suwansawat and Einstein 2007). The modern shield TBM is manufactured to simultaneously fill the tail void when the TBM is advancing. Due to this automation of shield TBM, the chamber pressure among the various operational parameters is a major factor to control the settlement. In EPBs TBM, the soil and water pressure in front of the cutter face is supported by the excavated soil inner a closed chamber. Therefore, the soil deformation due to the stress relief forwards the cutter face is restrained by the chamber pressure. The major factors to control the chamber pressure

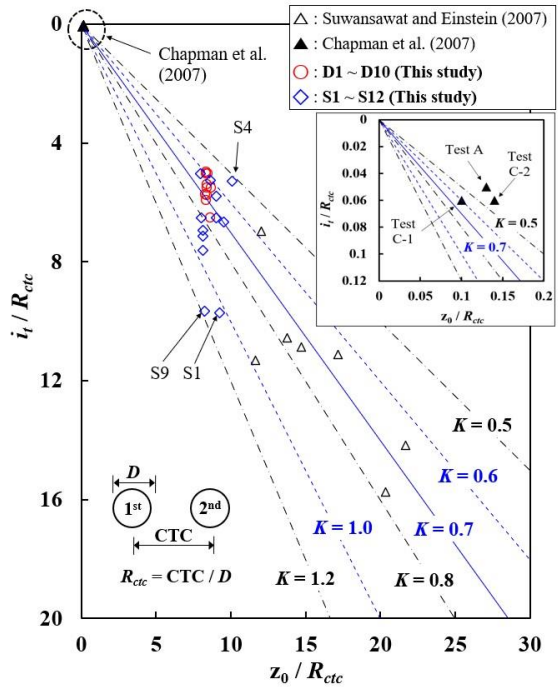

Fig. 12 Relationship between the parameters i and z_0 normalized by the centerline distance ratio (R_{ctc}). The measurements presented in this study are compared with the data from Bangkok MRTA project and model tests

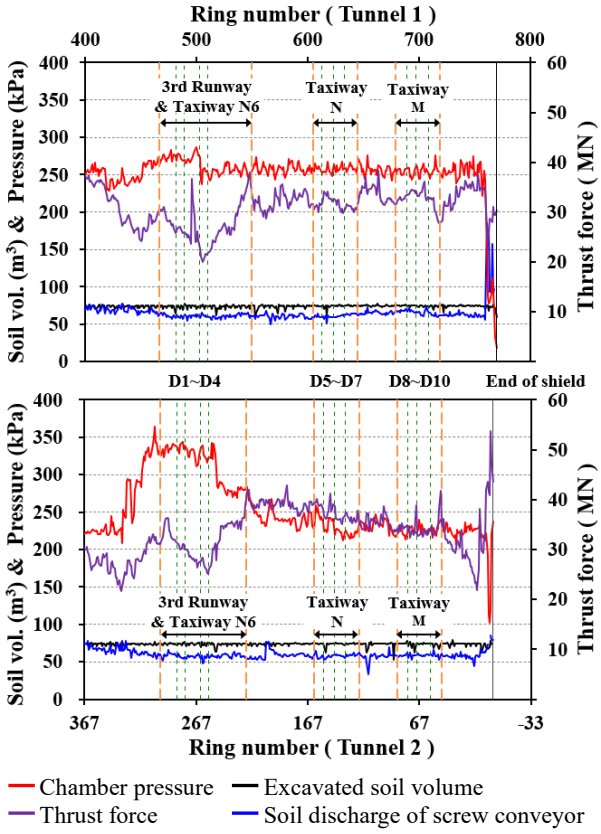

Fig. 13 Operating parameters of EPBs TBM

in EPBs TBM are the thrust force of shield jacks and the soil discharge of the screw conveyor.

The EPBs TBM operating parameters of the third runway and taxiway section in this project are shown in Fig. 13. A higher level of chamber pressure was applied when excavating the second tunnel under the runway compared with other sections because of the lower allowable settlement of the runway. As summarized in Table 4, the volume losses for section D1~D4 are significantly lower than those recorded in section D5~D10 for single tunnels, although similar chamber pressure was applied throughout the entire excavation. This demonstrates that the soil around section D1~D4 is stiffer compared to that around the other sections. When comparing the amount of increase in the volume loss when excavating the second tunnel, they are higher for section D1~D4 compared with those for section D5-D10, even though higher chamber pressure was applied when tunneling under the runaway. This shows that a direct correlation between the volume loss induced by the second tunnel and the chamber pressure cannot be established. It is revealed that the soil condition may have an important influence on the volume loss for the second tunnel. Further accumulation of the data is warranted to clarify the relationship between the chamber pressure and volume loss.

7. Conclusions

This paper presents a case study to characterize the surface settlement trough induced by twin tunnels excavated by EPBs TBM in sedimentary sand and clay strata underneath Incheon International Airport (IIA) in Korea. Because both the runway and taxiway were in operation during the under-crossing period, the surface settlements in the pavement zones were measured in detail in order to secure the safety of airport service. The settlement troughs after the first tunnel passings were recorded. After the tunnel was u-turned and the second tunnel was bored, the total settlement troughs were then measured. The additional settlement induced by the second shield passing was defined as the residual between the total settlement and that produced by the single tunnel.

- The surface settlement troughs induced by the first shield tunnel display symmetric shapes, whereas the additional settlement produced by the second shield tunnel displays marginal asymmetric shapes.
- The measured surface settlement troughs are approximated with Gaussian functions. The trough width parameter K of the settlement troughs produced by the first tunnel passings are determined, which are referred to as K_s. The additional settlement induced by the second tunnel passings are fitted with the asymmetric curves involving different parameters for near and remote limbs, denoted as K_n and K_r, respectively. The total settlement troughs are fitted both with a shifted symmetric Gaussian function with the parameter K_t and the superposition method utilizing the asymmetric function for the settlement trough produced by the second tunnel. The superposition method requires the definition of K_s, K_n, and K_r.
- It is demonstrated that the superposition method requiring three width parameters does not always yield a

more accurate prediction of the total settlement. Instead, the shifted symmetric Gaussian function using the parameter K_t is shown to result in better fits and favorable agreements with the recordings, when comparing the volume loss. The error rate is mostly within 10 % compared with the measurement. The normalized relation by R_{ctc} in Fig. 12 can be represented by a linear.

• The comparisons highlight that the shifted symmetric Gaussian function in twin shield tunnels is not only easier to use, but also provides a more reliable prediction of the settlement trough. It is therefore recommended to be used in practice for estimation of the settlement in clay caused by twin tunnelling.

• The amount of increase in the width parameter K_t for the twin tunnels relative to that for the single tunnel (K_s) is quantified with the K_t/K_s ratio. The mean ratio is 1.35 for this case study, whereas the mean value is 1.25 for the Bangkok MRT project. Considering the similarity of the ratios for two different projects constructed in different soils, a ratio of 1.3 is considered to be applicable for a preliminary estimate of the surface settlement trough for twin tunnels.

Acknowledgments

This study was supported by Korea Institute of Energy Technology Evaluation and Planning (KETEP), and the Ministry of Trade, Industry and Energy (MOTIE) of the Republic of Korea (No. 20183010025580).

References

Ahn, C.Y. (2017), "Railroad construction to connect the 2nd passenger terminal in Incheon Airport", Korean Tunnelling and Underground Space Association, Korea.

Arioglu, E. (1992), "Surface movements due to tunnelling activities in urban areas and minimization of building damages. Short Course, Istanbul Technical University", Mining Engineering Department. (in Turkish)

Attewell, P. and Farmer, I. (1974), "Ground deformations resulting from shield tunnelling in London Clay", *Can. Geotech. J.*, **11**(3), 380-395. https://doi.org/10.1139/t74-039.

Barratt, D.A. and Tyler, R.G. (1976), "Measurements of ground movement and lining behavour on the London Underground at Regents Park", Tunnels Division, Structures Department, Transportation and Road Research Laboratory 684, Crowthorne, Berkshire.

Chakeri, H., Ozcelik, Y. and Unver, B. (2013), "Effects of important factors on surface settlement prediction for metro tunnel excavated by EPB", *Tunnel. Underg. Space Technol.*, **36**, 14-23. http://doi.org/10.1016/j.tust.2013.02.002.

Chapman, D., Rogers, C. and Hunt, D. (2004), "Predicting the settlements above twin tunnels constructed in soft ground", *Tunnel. Underg. Space Technol.*, **19**(4/5), 378-380.

Chapman, D., Ahn, S. and Hunt, D.V. (2007), "Investigating ground movements caused by the construction of multiple tunnels in soft ground using laboratory model tests", *Can. Geotech. J.*, **44**(6), 631-643. https://doi.org/10.1139/t07-018.

Chen, R.P., Lin, X.T., Kang, X., Zhong, Z.Q., Liu, Y., Zhang, P. and Wu, H.N. (2018), "Deformation and stress characteristics of existing twin tunnels induced by close-distance EPBS under-crossing", *Tunnel. Underg. Space Technol.*, **82**, 468-481. https://doi.org/10.1016/j.tust.2018.08.059.

Chou, W.I. and Bobet, A. (2002), "Predictions of ground deformations in shallow tunnels in clay", *Tunnel. Underg. Space Technol.*, **17**(1), 3-19. https://doi.org/10.1016/S0886-7798(01)00068-2.

Della Valle, N. and Rodríguez, M.M. (2014), "Twin tunnels and asymmetrical settlement troughs in soft soils", *World Tunnel Congress 2014*, Brazil.

Ding, Z., Wei, X.J. and Wei, G. (2017), "Prediction methods on tunnel-excavation induced surface settlement around adjacent building", *Geomech. Eng.*, **12**(2), 185-195. http://doi.org/10.12989/gae.2017.12.2.185.

Djelloul, C., Karech, T., Demagh, R., Limam, O. and Martinez, J. (2018), "2D numerical investigation of twin tunnels-Influence of excavation phase shift", *Geomech. Eng.*, **16**(3), 295-308. https://doi.org/10.12989/gae.2018.16.3.295.

Fargnoli, V., Boldini, D. and Amorosi, A. (2015), "Twin tunnel excavation in coarse grained soils: Observations and numerical back-predictions under free field conditions and in presence of a surface structure", *Tunnel. Underg. Space Technol.*, **49**, 454-469. http://doi.org/10.1016/j.tust.2015.06.003.

Glossop, N.H. (1978), "Soil deformations caused by soft-ground tunnelling", Durham University.

Herzog, M. (1985), "Surface subsidence above shallow tunnels", *Bautechnik*, **62**(11), 375-377.

Hunt, D. (2005), "Predicting the ground movements above twin tunnels constructed in London Clay", University of Birmingham Birmingham.

Jin, D., Yuan, D., Li, X. and Zheng, H. (2018), "An in-tunnel grouting protection method for excavating twin tunnels beneath an existing tunnel", *Tunnel. Underg. Space Technol.*, **71**, 27-35. http://dx.doi.org/10.1016/j.tust.2017.08.002.

Kim, D., Pham, K., Park, S., Oh, J.Y. and Choi, H. (2020), "Determination of effective parameters on surface settlement during shield TBM", *Geomech. Eng.*, **21**(2), 153-164. https://doi.org/10.12989/gae.2020.21.2.153.

Korea-National-Railway (2013), "Railroad construction to connect the 2nd passenger terminal in Incheon International Airport", 226311C10-308-001, K.N. Railway.

Li, X. and Yuan, D. (2012), "Response of a double-decked metro tunnel to shield driving of twin closely under-crossing tunnels", *Tunnel. Underg. Space Technol.*, **28**, 18-30. https://doi.org/10.1016/j.tust.2011.08.005.

Liao, S.M., Liu, J.H., Wang, R.L. and Li, Z.M. (2009), "Shield tunneling and environment protection in Shanghai soft ground", *Tunnel. Underg. Space Technol.*, **24**(4), 454-465. https://doi.org/10.1016/j.tust.2008.12.005.

Mair, R. and Taylor, R. (1997), "Theme lecture: Bored tunnelling in the urban environment", *Proceedings of the Fourteenth International Conference on Soil Mechanics and Foundation Engineering*, Rotterdam.

Mair, R.J. (1979), *Centrifugal Modeling of Tunnel Construction in Soft Clay*, Cambridge University.

Mair, R.J., Taylor, R.N. and Bracegirdle, A. (1993), "Subsurface settlement profiles above tunnels in clays", *Geotechnique*, **43**(2), 315-320. https://doi.org/10.1680/geot.1993.43.2.315.

McCabe, B., Orr, T., Reilly, C. and Curran, B. (2012), "Settlement trough parameters for tunnels in Irish glacial tills", *Tunnel. Underg. Space Technol.*, **27**(1), 1-12. https://dx.doi.org/10.1016/j.tust.2011.06.002.

Nawel, B. and Salah, M. (2015), "Numerical modeling of two parallel tunnels interaction using three-dimensional Finite Elements Method", *Geomech. Eng.*, **9**(6), 775-791. http://doi.org/10.12989/gae.2015.9.6.775.

New, B. and Bowers, K. (1994), "Ground movement model validation at the Heathrow Express trial tunnel", *Tunnelling'94*,

Springer.
O'reilly, M. and New, B. (1982), "Settlements above tunnels in the United Kingdom; their magnitude and prediction", https://eurekamag.com/research/020/004/020004527.php.
Peck, R.B. (1969), "Deep excavations and tunneling in soft ground", *Seventh International Conference on Soil Mechanics and Foundation Engineering*, Sociedad Mexicana de Mecanica de Suelos, A.C., Mexico City, Mexico.
Rankin, W.J. (1988), "Ground movements resulting from urban tunnelling: Predictions and effects", *Geolog. Soc., London, Eng. Geol. Spec. Public.*, **5**(1), 79-82.
Sirivachiraporn, A. and Phienwej, N. (2012), "Ground movements in EPB shield tunneling of Bangkok subway project and impacts on adjacent buildings", *Tunnel. Underg. Space Technol.*, **30**, 10-24. https://doi.org/10.1016/j.tust.2012.01.003.
Stallebrass, S., Springman, S. and Love, J. (1992), "Recollections from the wroth memorial symposium: Predictive soil mechanics", *Predictive Soil Mechanics: Proceedings of the Wroth Memorial Symposium*, St Catherine's College, Oxford, July.
Suwansawat, S. and Einstein, H.H. (2007), "Describing settlement troughs over twin tunnels using a superposition technique", *J. Geotech. Geoenviron. Eng.*, **133**(4), 445-468. https://doi.org/10.1061/(ASCE)1090-0241(2007)133:4(445).
Xu, Q., Zhu, H., Ding, W. and Ge, X. (2011), "Laboratory model tests and field investigations of EPB shield machine tunnelling in soft ground in Shanghai", *Tunnel. Underg. Space Technol.*, **26**(1), 1-14. https://doi.org/10.1016/j.tust.2010.09.005.
Zapata, S.F. (1998), "Prediction and field observation in soft ground tunnel", Illinois Institute of Technology.
Zhao, W., Jia, P.J., Zhu, L., Cheng, C., Han, J., Chen, Y. and Wang, Z.G. (2019), "Analysis of the additional stress and ground settlement induced by the construction of double-o-tube shield tunnels in sandy soils", *Appl. Sci.*, **9**(7), 1399. https://doi.org/10.3390/app9071399.

GC